ARCADA

Biofilm prevention on 3D printed surfaces for biomedical applications

Denise Nurmi

Degree Thesis

Materials Processing Technology

2020

DEGREE THESIS	
Arcada	
Degree Programme:	Materials Processing Technology
Identification number:	21545
Author:	Denise Nurmi
Title:	Biofilm prevention on 3D printed surfaces for biomedical applications
Supervisor (Arcada):	Stewart Makkonen-Craig
Supervisor (University of Helsinki)	Cristina Durante Cruz
Commissioned by:	

Abstract:

Biofilms are complex communities of bacteria residing within an exopolysaccharide matrix that adheres to a surface, such as medical devices and implants, causing chronic infections. Due to the antibiotic resistant nature of biofilms, the use of antibiotics alone is ineffective for treating biofilm-related infections. Hydrophilicity plays an important role in surface attachment because the first step for biofilm formation is bacterial adhesion to a surface and biofilm is less likely to form on hydrophilic surfaces. In this thesis, biofilm formation inhibition of *Staphylococcus aureus* on 3D printed modified surfaces was investigated. Modifications included: treatment of polylactic acid and thermoplastic polyurethane filaments with polyethylene glycol and castor oil, as well as surface polishing. Samples were tested for wettability by the contact angle method and surface changes were analyzed microscopically. Wettability of treated samples increased, except for polished thermoplastic polyurethane. All samples were decontaminated before the microbiological assays were performed. Four decontamination methods were tested (immersion in 70% ethanol for 15 minutes only and combined with vortex, autoclavation and ultraviolet germicidal irradiation). Autoclaving was an efficient sterilization method; however, this process affected the surface of the samples. Ultraviolet germicidal irradiation was an optimum decontamination step. Biofilm growth inhibition was analyzed through the resazurin method. Four out of six treated samples inhibited biofilm formation at different levels. Polished thermoplastic polyurethane and polished polylactic acid samples inhibited biofilm formation by 47% ($\pm$ 6) and 33% ($\pm$36), respectively. Polylactic acid-polyethylene glycol had the most significant antibiofilm property by reducing biofilm formation by 52% ($\pm$5), followed by 22% ($\pm$12) in polylactic acid-castor oil. Based on these preliminary data, polished surfaces and filaments treatment with polyethylene glycol showed promising results for biofilm inhibition.

Keywords:	3D printing, bacterial biofilm, polylactic acid, thermoplastic polyurethane, hydrophilic surface, contact angle
Number of pages:	54
Language:	English
Date of acceptance:	

Abbreviations

3D	Three dimensional
CA	Contact angle
FDM	Fused deposition modelling
FU	Fluorescence unit
PLA	Polylactic acid
TPU	Thermoplastic polyurethane
TSBG	Tryptic Soya Broth supplemented with glucose
UVGI	Ultraviolet germicidal irradiation

CONTENTS

Figures

Tables

AKNOWLEDGEMENTS

1   INTRODUCTION

1.1   Background

Although 3D printing is not a new technology, it only became popular in the medical industry over the last few years. The medical field is the fastest growing area utilizing 3D printing technique. The ability to accelerate personalized care and the possibility to use low cost biocompatible polymers has made 3D printing technology a promising choice for manufacturing implants and other medical devices. However, the common practices of hospital sterilization can degrade polymers (Kerns 2019), leading to premature device failure. Neches et al. (2016) observed that whilst most 3D printed objects cannot be autoclaved, 3D printing machines use temperatures higher than autoclave cycles to extrude polymers and therefore, 3D printing objects are sterile. Despite this, general hygiene and asepsis are not effective methods for preventing biofilm formation on the surface of biomedical devices (Brisset et al. 1996).

A biofilm provides the bacterial colony with strong antibiotic resistance. Räsänen (2018) observed that bacteria present in a biofilm are 10 to 1,000 times more resistant to antibiotics in comparison to free-floating (planktonic) bacteria. Both Gram-positive and Gram-negative bacteria can form biofilms on medical devices and can become life threatening, leading to device failure, chronic infections and high mortality and morbidity rates (Khatoon et al. 2018). According to Chen et al. (2013), it is estimated that *Staphylococcus aureus* and *S. epidermidis* cause about 50–70 % of catheter and implantable device biofilm-related infections. Further to this, "the risk of developing a catheter-associated infection increases by approximately 10 % each day the catheter is in place" (Percival et al. 2015).

Therefore, medical devices should have properties that prevents the initial attachment of bacteria, which will as a result, hind biofilm formation and inhibit the insurgence of antibiotic resistant bacteria.

1.2 Aims and objectives

The aims of this thesis were to develop strategies that improve hydrophilicity of 3D printed samples and evaluate their effects on the biofilm growth of *S. aureus*. Other objectives included:

- Analyze changes in surface energies using the contact angle method and optical microscopy in order to select optimum surface modification strategy.

- Find an effective surface decontamination method that does not interfere with the material's properties and treatment applied.

Chapter 2 of this thesis describes the literature review done in order to have a better understanding on bacterial biofilm formation and how it can be prevented on surfaces of biomedical devices. Chapter 3 provides the methodology and data collection process. Chapter 4 presents the results obtained through different treatments, sample sterilization and biofilm inhibition. Chapter 5 is dedicated to evaluation of the results. Chapter 6 provides the conclusion of this work. In summary, the thesis follows the steps seen in Figure 1. Samples were 3D printed in the chemistry laboratory of Arcada UAS and biofilm analysis was done at the University of Helsinki, Faculty of Pharmacy.
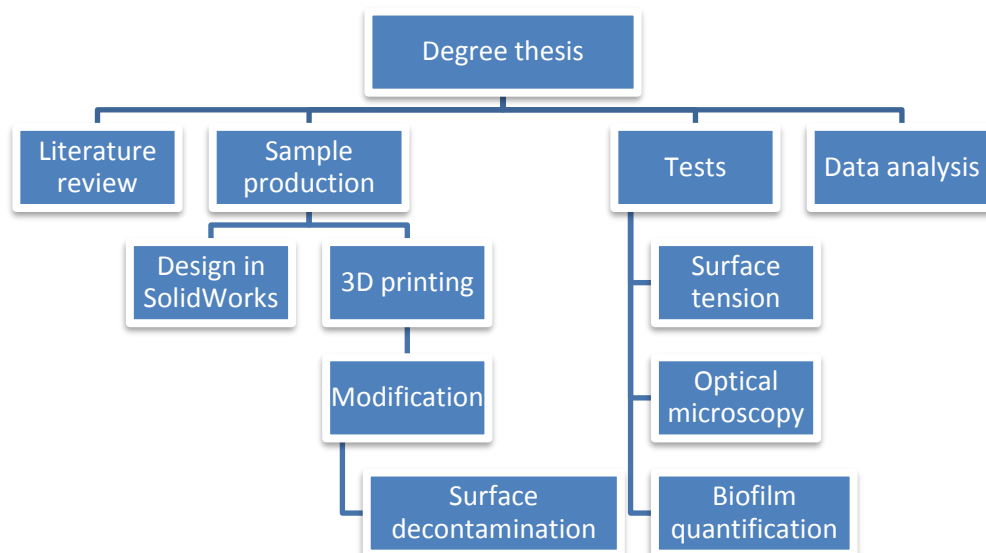
Figure 1. Flow chart of project structure.

2 LITERATURE REVIEW

2.1 Bacterial biofilm

2.1.1 Biofilm characteristics and formation

Bacterial biofilm consists of a community of living cells involved in an extracellular polymeric matrix and adhered to a surface (Bjarnsholt 2011). The polymeric substance is produced by the microorganisms, present in the biofilm, in order to increase their chance of survival. Bacteria move to a material surface by the effects of physical forces, such as Brownian motion, van der Waals attraction forces, gravitational forces, the effect of surface electrostatic charge and hydrophobic interactions (Katsikogianni and Missirlis 2004).

Biofilm formation is a cyclic process, and follows five stages (Figure 2):
(1) initial attachment, (2) irreversible attachment, (3) maturation I stage, (4) maturation II stage and (5) dispersion stage.
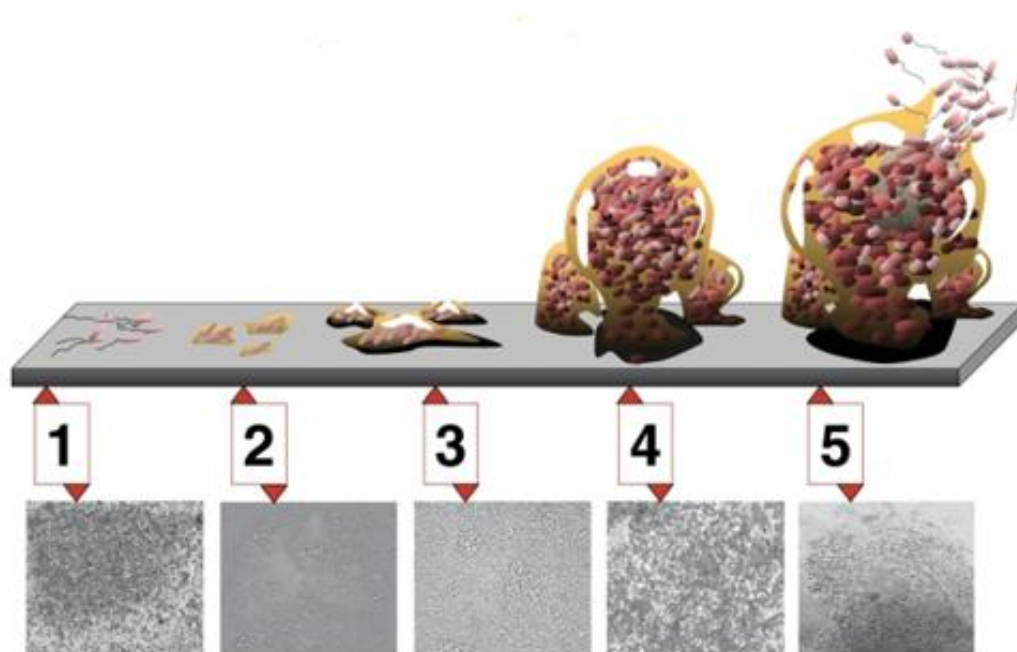
Figure 2. Stages of biofilm formation (Monroe 2007).

In the initial phase, the attachment of bacteria to a surface is determined by physical and chemical interactions (Katsikogianni and Missirlis 2004). Within hours, bacteria start to multiply and microcolonies are stablished. When microcolonies are formed, the attachment becomes irreversible. After 24 hours occurs the maturation phase, when microcolonies increase in size and form new cell layers that covers entirely the surface. As cells divide, the density and complexity of the biofilm increase. The last phase is when the biofilm reaches its dynamical equilibrium, usually within 48 hours of infection (Donlan and Costerton 2002) and it is also when the outer layers of the biofilm release cells. This phase is crucial for spreading infection, since it is when bacteria expand to other regions of the body causing chronic infections and embolic complications (Khatoon et al. 2018).

The Gram-positive bacteria *S. aureus and S. epidermidis* are the most common causes related to hospital-acquired infections on medical devices (Otto 2008). A clinical research study conducted by Chu et al. (2005) shows that infection related to *S. aureus* has a significant impact on patients with prosthetic devices, where 41% presented complications leading to death of 27% of patients. Examples of hospital-acquired infections on medical devices are shown in Table 1.

Table 1. Types of polymeric medical devices associated with nosocomial infections (Polívková et al. 2017)

Bacterial species	Medical device categories	Example medical devices
Staphylococci, *Enterobacteriaceae* and Enterococci	Catheters	Blood vessel catheter, CAPD catheters
	Tubes	Cerebrospinal fluid shunts, endotracheal tubes
	Cardiological implants	Arterial grafts, cardiac valves, pacemaker electrodes, total artificial hearts
	Prosthesis	Total joint replacements, ocular and penile prostheses
Enterobacteriaceae and Enterococci	Urinary catheters	Transurethral, suprapubic, and nephrostomy catheters
	Urinary stents	Double-J stents

2.1.2 Biofilm prevention

Bacteria can easily attach on the surface of biomedical devices and they are the culprit of significant morbidity and mortality among patients (Chen et al. 2013). One of the approaches that has been used to prevent biofilm formation is the use of antibiotic coatings on biomedical devices (Chemaly et al. 2010). However, Chang (as cited in Khatoon et al. 2018) noted that the extracellular polymeric substance secreted by bacterial biofilm is responsible not only for protecting itself against antibiotics, but it is also a scaffold for surface attachment. It can select for antibiotic resistant bacteria, thus other interventions are needed (Hoffman et al. 2005).

Cattò and Cappitelli (2019) observed that preventive strategies have been addressed in the last 20 years as alternatives to the use of bactericides. The development of polymeric materials that can prevent or weaken bacterial attachment is a promising approach to reduce material-associated biofilm problems (Alves and Pereira cited in Cattò and Cappitelli 2019). Bacterial adherence can occur preoperatively or postoperatively, and it depends on the physicochemical characteristics of the surface (Francolini and Donelli 2010). Surface hydrophilicity, charge, roughness, and topographical configuration can diminish bacterial adhesion and as result, prevent biofilm formation. (Achinas et al. 2019).

Surface free energy plays an important role in determining the adhesion of bacteria; biofilm is less likely to form on hydrophilic surfaces (Di Ciccio et al. 2015). However, materials commonly used in biomedical applications, such as polylactic acid (PLA) and polyurethane (PU), typically present relatively low surface energies.

Different approaches can be chosen to change the surface energy of a material. Ouyang et al. (2009) observed that the synthesis of polyethylene glycol (PEG) and PLA through melt polymerization increased hydrophilicity considerably. Noorisafa et al. (2016) successfully decreased the hydrophobicity of polyurethane through a PEG grafting technique. Furthermore, polymers subjected to polishing procedures decrease their contact angle (CA) according to a study conducted by Namen et al. (2008), which as a result, increased their surface energy. Another study shows that CA decreased notably after polymer films were impregnated with vegetable oil (Mukherjee et al. 2018).

2.2 3D printing

2.2.1 Principles of 3D printing

3D printing, also known as additive manufacturing, is revolutionizing the technological, medical and food industry with the new approach to build things. 3D printing technique has developed considerably in the last 15 years with the introduction of new printing materials (Dimitrov et al. 2006). This technique benefits the environment by reducing waste material (Ford and Despeisse 2016) and therefore, reduces carbon emissions. In addition, because of the size of the 3D printing machine and the variety of materials it can print, many printers can be installed in smaller places. Figure 3 shows the working mechanism of a 3D printer that uses the Fused Deposition Modeling (FDM) technique.

Filament is loaded
to the extruder

The extruder is able
to control the amount
of filament precisely

The system moves the extruder head
to be in position for printing the next layer

The hot end melts the
filament to be fluid in state

The object is being
constructed
layer by layer

Heat bed
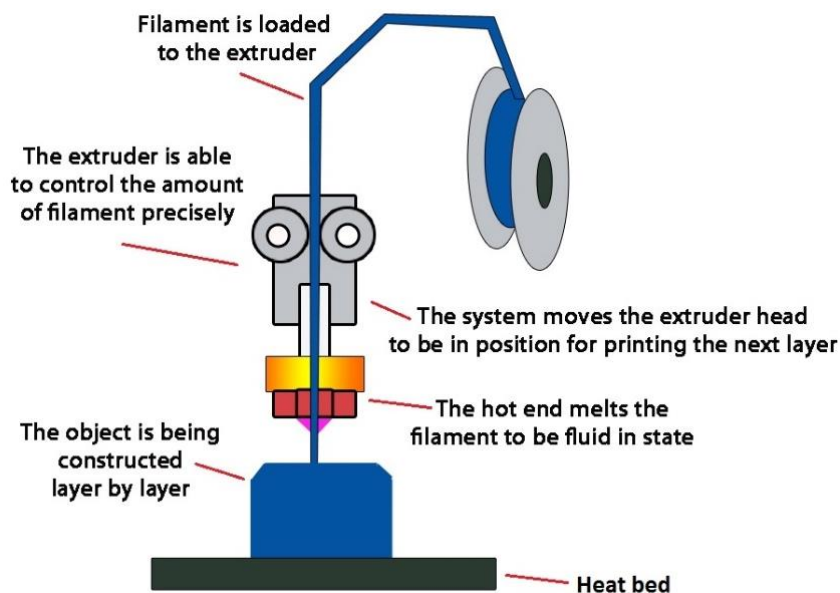
Figure 3. Working mechanisms of a 3D printer (Ozeki n.d.).

The mechanical strength of an object can be improved by modifying how the internal layers are constructed. High infill coverage percentage corresponds to a more resistant object. 3D printing software offers a number of options ranging from different infill patterns and coverage percentage (Figure 4) that can be applied depending on the end use of the 3D printed object.
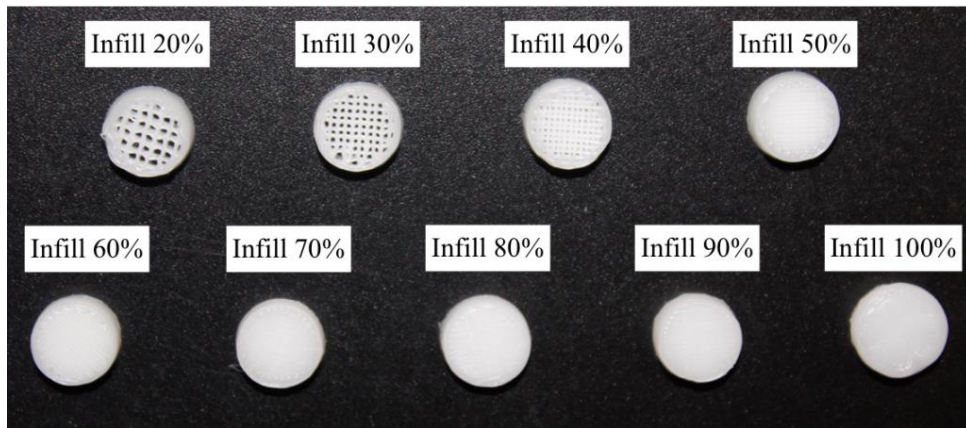
Figure 4. Pore size variations by infill percentage changes (3D@UniPV n.d.).

2.2.2 Printing materials

2.2.2.1 Polylactic acid

PLA is a non-toxic, biodegradable and biocompatible polymer derived from renewable resources widely used to produce 3D objects by fused deposition modelling (Liu et al. 2019). PLA can be produced by direct polycondensation or by ring-opening polymerization (Sin and Tueen 2019). Figure 5 shows the chemical structure of PLA.
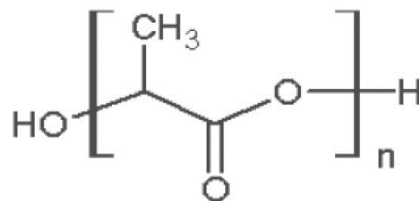
Figure 5. Polylactic acid chemical structure. (Singh 2011)

PLA was approved by the US Food and Drug Administration in 1970 to be used in direct contact with biofluids (Singhvi, Zinjarde and Gokhale 2019). Due to its mechanical properties and biocompatibility, PLA became a good choice for medical applications. However, PLA is relatively hydrophobic, with water CA between 75º - 85º (Baran and Erbil 2019), which makes a favorable environment for the formation of bacterial biofilm.

2.2.2.2 *Thermoplastic Polyurethane*

TPU is a flexible and high resistance heterogeneous synthetic polymer first developed in the 1950s (Vizzeswarapu 2014). TPU presents hydrophobic characteristics (Villani et al. 2020), and it has hygroscopic behavior (Xiao and Gao 2017). Its structure is made of a copolymer block of hard and soft segments (Figure 6).
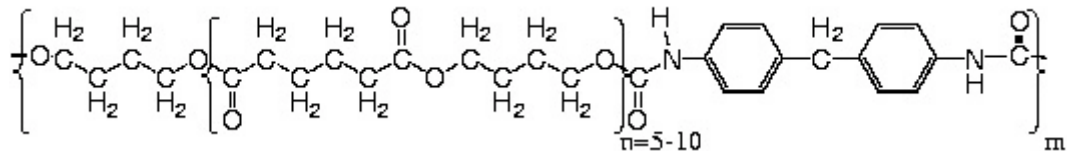
Figure 6. Thermoplastic polyurethane structure (Omnexus n.d.).

TPU is one of the most versatile polymers available for biomedical applications because of its high tensile strength, toughness, abrasion and degradation resistance and excellent biocompatibility and biostability (Rajan et al. 2013). Additionally, medical grade TPU does not contain rubber accelerator and plasticizers, which does not cause skin dermatitis or irritation (Vizzeswarapu 2014). TPU has a promising application in the medical field and it includes fabrication of customized implants and scaffolds for rehabilitation, human bone techniques, and drug delivery devices (Xiao and Gao 2017).

2.3 Surface characterization techniques

2.3.1 Contact angle

The surface energy of a solid material can be calculated by testing different liquids and measuring its CA. CA is used to verify the intensity of the phase contact between liquid and solid substances: coating, painting, cleaning, printing, hydrophobic or hydrophilic coating and bonding (Krüss n.d.). The wettability of surfaces depends on the thermodynamic equilibrium of solid, liquid and gas. Therefore, CA is a quantitative means of the wettability process and can be calculated using Eq. (1).

$$\gamma_{SV} - \gamma_{SL} = \gamma_{LV} \times cos\,\theta \qquad\qquad (1)$$

Young (1805) observed that a liquid resting on a surface is subjected to three surface tensions (Figure 7): at the interfaces of the liquid and vapor (γ_{LV}), solid and liquid (γ_{SL}) and solid vapor (γ_{SV}) phases.
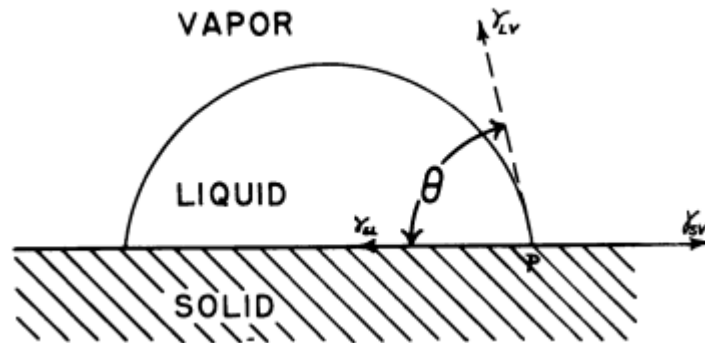
Figure 7. Contact angle of a sessile drop (Zisman 1964).

On a low energy surface, liquids will not be able to wet the surface and the surface tension will result in a high CA. When the surface energy is high, liquids will tend to flatten out with a low CA (Huhtamäki et al. 2018). The surfaces can be defined as: superhydrophilic (CA< 10º); hydrophobic (CA > 90º); hydrophilic (CA < 90º) and superhydrophobic (CA >150º).

CA alone is not a direct indicator of chemical or physical changes of the surface, however, hydrophilicity is a relevant surface characterization when testing adhesion of bacterial biofilm. Because the first step for biofilm formation is bacterial adhesion to a surface, hydrophobicity plays an important role in surface attachment (Di Ciccio et al. 2015).

2.3.2 Optical Microscopy

An optical microscope, also known as light optical microscope, uses visible light and a system of lenses to magnify small objects (Gianfrancesco 2017). The main components of an optical microscope are: condenser (controls the focus and position of the light), diaphragm (controls the size and intensity of the light), illuminator (transmits light through a translucent object), objective lens (controls the resolution of the image) and ocular lens (improves the resolution by further magnifying the image) (Figure 8).

17
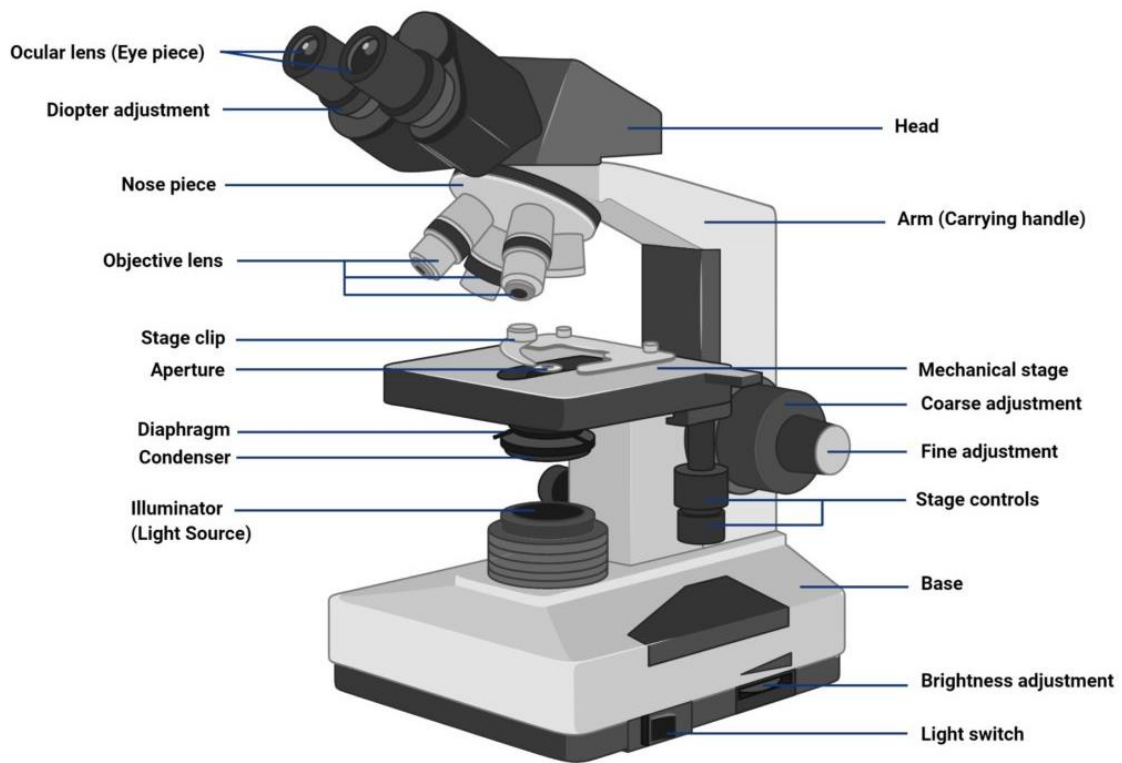
Figure 8. Parts of an optical microscope (Aryal 2020).

Surface characterization can be done with a white-light to a resolution of 0.2 µm and it is possible to observe the surface morphology, color, opacity, and optical properties of a material (Kazuhisa, 2002).

3 EXPERIMENTAL PROCEDURES

In this section, the experimental procedures are presented focusing on the aims and objectives of this thesis and are based on scientific publications described in Chapter 2. A detailed explanation of 3D printing of the samples, their respective treatments to improve hydrophilicity, decontamination processes and biofilm inhibition assessment will be described. The methods used for surface characterization and data analysis will also be provided in this chapter.

3.1 Materials and methods

3.1.1 3D printed samples

The first step of this study was to choose appropriate filaments for 3D printing. PLA and TPU filaments were chosen based on their biomedical applications compatibility. Industrial transparent PLA (BQ F000148 Easy Go) and TPU (Formfutura Python Flex™ Clear) Ø 1.75 mm filaments were purchased from 3D Jake. A 3D printer (Creality CR-10) was used to produce the samples.

Defining sample dimensions was another important aspect to take into consideration. Samples should have suitable dimensions to fit in a 24-well plate. Five different sample sizes were designed in SolidWorks 2019 and 3D printed with PLA to verify which one would best suit for further use during the microbiological assays: **1.** 10 mm (diameter) x 1 mm (height), **2.** 10 mm x 2 mm, **3.** 10 mm x 3 mm, **4.** 20 mm x 2 mm and **5.** 20 mm x 3 mm.

The SolidWorks designs of the samples were converted into 2D slices using CURA software. To enhance mechanical strengths, 100% infill and triangle pattern were used to build the internal layers of the samples. Other 3D printing parameters where set according to the manufacturer recommendation for printing with the chosen filaments.

To improve sample removal from the build plate, the printing surface was prepared with a printer tape. A filament spool was installed to the printer and loaded into the extruder.

The extruder was heated to 205 °C. Melted filament was deposited to the build plate creating successive layers as seen in Figure 9.
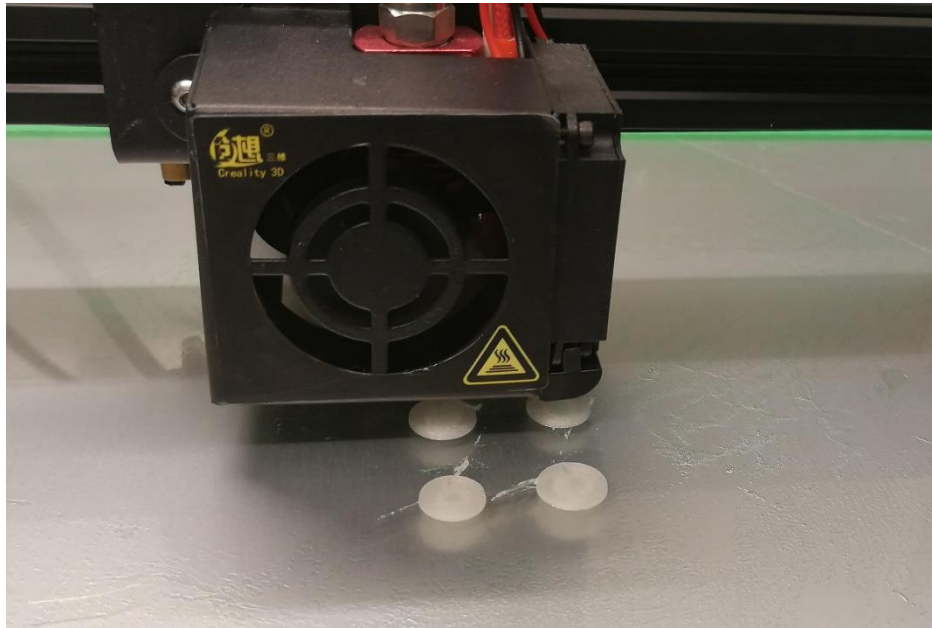
Figure 9. Sample printing.

The 3D printed samples size suitability was assessed based on the well dimensions of a 24-well plate and forceps manipulation. If the sample was too thick, more resazurin would be needed for biofilm quantification. In contrast, if the sample was too thin or too wide, the use of forceps for the manipulation of samples would be a challenge. The ones that were suitable for this study were 3D printed with PLA and TPU. 3D printing of control samples followed the same parameters as described above. However, the extruder was heated to 240 °C when printing with TPU filament.

3D printed samples to be used for surface polishing treatment were produced using ironing feature available in CURA software during the last part of the printing process to decrease top layer roughness.

3.1.2 3D printed sample holder

In order to polish the samples, a holder was modeled in SolidWorks. The model consists of a 13 mm circle that was extruded to the height of 15 mm (Figure 10a). A 10 mm circle was used to create the cavity to attach the sample that was cut from the top of the model to the depth of 1.5 mm. This enables the sample to stay in place while being subjected to

mechanical forces during polishing process. An 8 mm circular cavity was cut into the full-length of the model, to not only save material, but also to facilitate the use of tools if the sample would get stuck in the holder. The 3D design was converted into 2D slices in CURA software and 3D printed with TPU filament (Figure 10b). Sample holder was tested to verify if it needed further adjustments (Figure 10c).
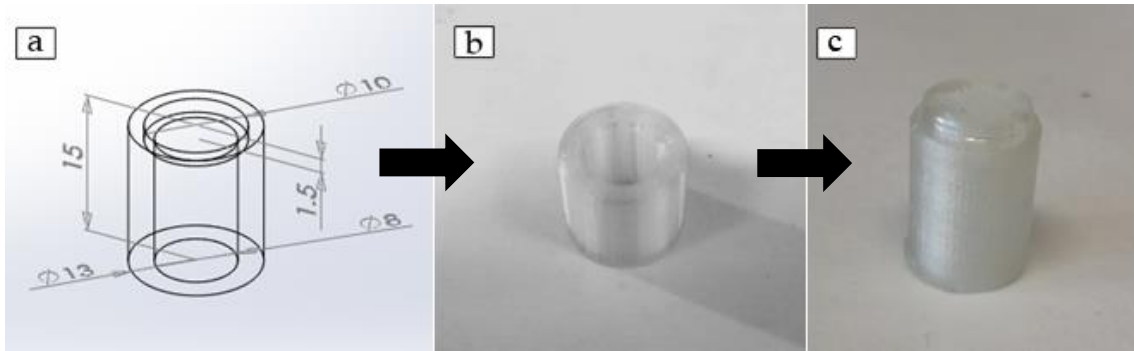
*Figure 10. Sample holder (**a**) technical drawing, (**b**) 3D printed and (**c**) with a sample attached.*

3.1.3 Treatments

3.1.3.1 Additives

- Filaments treated with PEG

Approximately 1.5 m of PLA and TPU filaments were immersed in PEG 400 for 24 hours in Petri dishes (Figure 11). Excess of PEG was removed with dust-free paper. Filaments were weighted, and samples were 3D printed using the parameters as described in 3.1.1.

- Filaments treated with castor oil

Approximately 1.5 m of PLA and TPU filaments were immersed in castor oil (HAUT-SEGALA) for 24 hours in Petri dishes (Figure 11). Excess castor oil was removed with dust-free tissue paper. Filaments were weighed, and samples were 3D printed using the parameters described in 3.1.1.
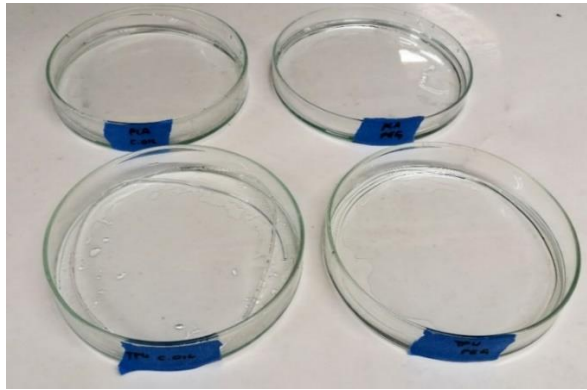
Figure 11. Filaments treated with castor oil and PEG.

3.1.3.2 Surface polishing

PLA and TPU samples with the thickness of 3 mm were subjected to surface removal followed by surface polishing in a polishing machine, Innovation 200M (Remet) (Figure 12a) using discs of 320 – 4000 grit.

Samples were attached to a 3D printed sample holder (Figure 9c) and were polished at a rotation speed of 300 rpm using planar motion according to time and grit size seen in Figure 12b. To minimize heat friction and to remove dust, running cold water was used to rinse the discs during the polishing procedure. Microscopy analysis was done after every grit use to ensure that the surface was getting smoother.
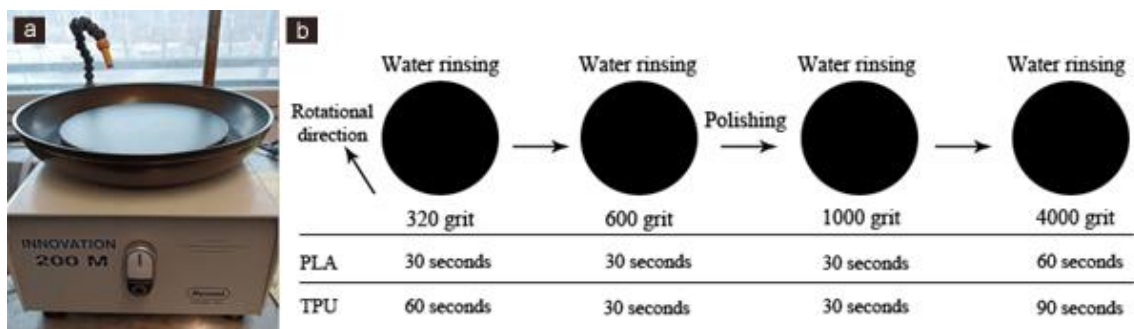
Figure 12. Polishing (a) apparatus (b) procedure

3.1.4 Decontamination methods

Four decontamination methods based on a study conducted by Neches et al. (2016) were tested. The experiments were carried out inside a Biosafety class II cabinet to ensure a sterile environment.

3.1.4.1 Ethanol

Samples were transferred to a test tube and were immersed for 15 minutes in 5 mL of 70% ethanol, following by drying in room temperature inside Biosafety class II cabinet for seven and half minutes each side (Figure 13).
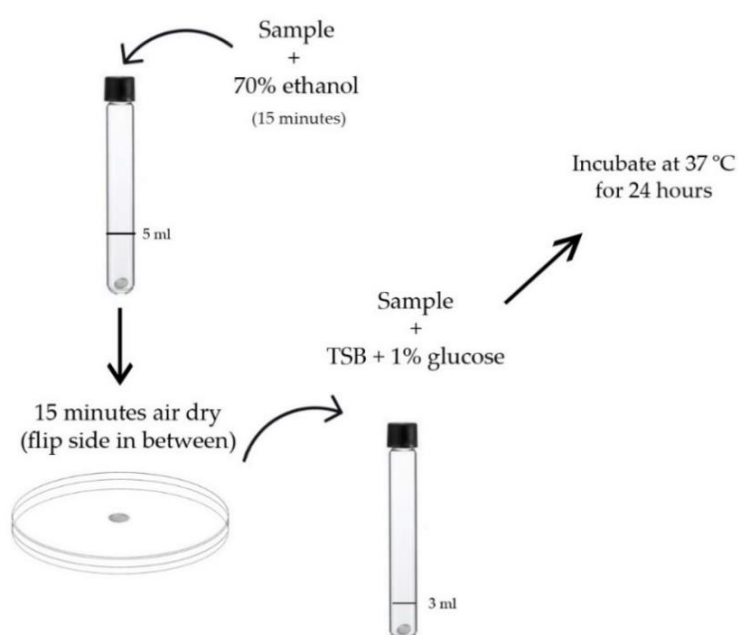
Figure 13. Ethanol decontamination protocol.

3.1.4.2 Ethanol + vortex

Samples were immersed for 15 minutes in a 5 mL solution of 70% ethanol in a test tube and were vortexed every five minutes for 10 seconds. Samples were then air-dried in room temperature inside Biosafety class II cabinet for seven and half minutes each side.

3.1.4.3 Autoclave

Samples were placed into sealed packages individually and autoclaved for 15 minutes at 121 ℃. This was performed by authorized personnel at Faculty of Pharmacy, University of Helsinki.

3.1.4.4 Ultraviolet germicidal irradiation

Ultraviolet germicidal irradiation (UVGI) was done by exposing each side of the surface of the samples to mercury-based UV light at wavelength of 250 nm for 30 minutes each side, inside a Biosafety class II cabinet.

After being exposed to all decontamination methods described above, samples were transferred to sterile test tubes containing Tryptic Soya Broth supplemented with 1% glucose (TSBG) and incubated at 37 ℃ for 24 hours. Turbidity was verified by eye, which indicates bacterial growth, thus failure of the process. Surface energy (CA measurement) was done in each sample and microscopy analysis was done for samples subjected to ethanol and ethanol with vortexing, as well autoclave sterilization methods, to evaluate any changes that the process may have caused on samples properties.

3.1.5 Microbiological assays

The experiments were organized into two sections and were performed according to a protocol used by Cruz, Shah and Tammela (2018).

3.1.5.1 Biofilm formation
S. aureus (ATCC 29213; PML Microbiologicals®) was cultured in Tryptic Soya Agar (TSA) plates at 37 °C for 24 hours (Figure 14).
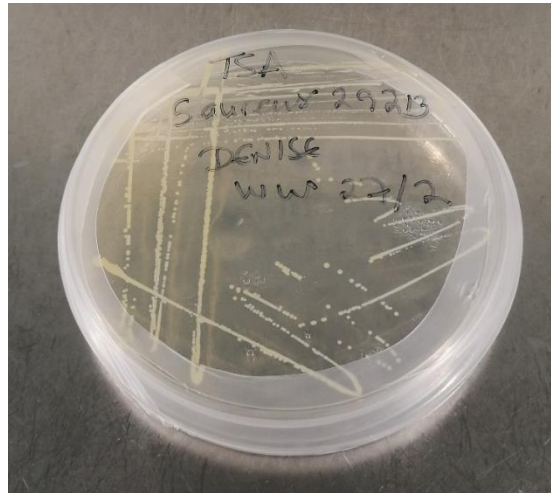
Figure 14. Staphylococcus aureus culture.

Five colonies from TSA overnight culture were added into a test tube containing 5 mL of 0.9% saline solution. Turbidity was measured in a densitometer (DEN-1, BioSan) and bacterial suspension was adjusted using McFarland standards, according to 5 x 10^5 colony forming units (CFU/mL) in TSBG. TSBG has previously been shown to be an optimal medium for biofilm growth of *S. aureus* (Cruz, Shah and Tammela 2018).

Samples were placed in a 24-well plate, with the treated surface up, using sterile forceps, following the layout seen in Figure 15. Then 1 mL of bacterial suspension, prepared as describe above, was added to each well, except in the control wells located on Row D, where 1 mL of sterile TSBG was added. Samples were submerged to the bottom of the plate with the aid of a pipette tip to ensure that treated surface of samples were covered by the bacterial suspension. The plate was incubated at 37 °C for 24 hours.
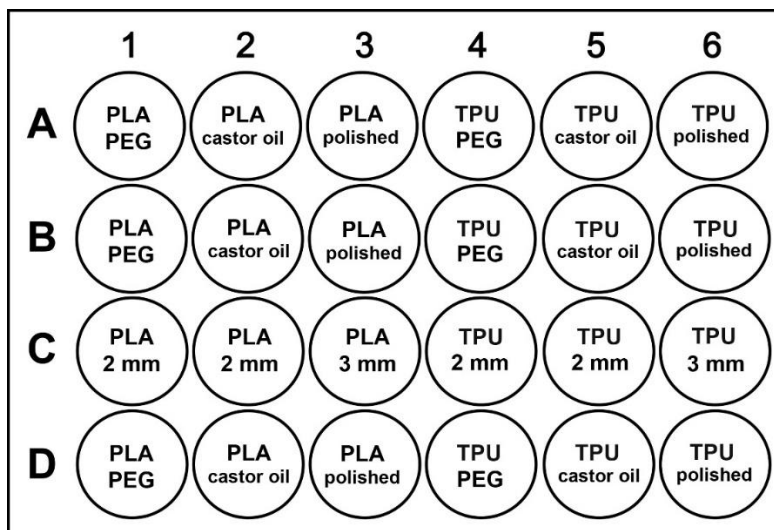
Figure 15. Plate layout.

3.1.5.2 Biofilm quantification

Biofilm quantification was done using resazurin as a quantification method of microorganisms of *S. aureus* present on the biofilm. After biofilm was formed on the surfaces, samples were washed twice with phosphate buffered saline (PBS). Removal of media and washing steps with PSB solution (twice) was performed using an automatic aspiration system (low speed to avoid biofilm disruption). Samples were then transferred to a sterile 24-well plate using sterile forceps.

A 4 µg/mL solution of resazurin (Sigma) was prepared in PBS and 1 mL of this solution added into each well containing the sample. The plate was then incubated at 25 ºC for 20 minutes. An aliquot of 100 µL of the sample solution was transferred, in duplicate, to a new sterile 96-well plate. Antibiofilm properties of the surfaces were evaluated by measuring the fluorescence produced by resazurin at wavelengths of 530 nm excitation and 590 nm emission using Varioskan Ascent (Labsystems International).

3.2 Surface test methods

3.2.1 Wettability analysis

Surface wetting characterization of treated and non-treated samples was done through sessile drop technique at 21±1 ℃. A basic setup for CA analysis was prepared for the experiment according to Figure 16. A drop of distilled water was pipetted on the sample and a digital photograph was taken. The test was repeated in triplicate for each sample. CA was optically measured through geometrical analysis of the picture using ImageJ software. The average values of the three measurements of each sample were calculated.
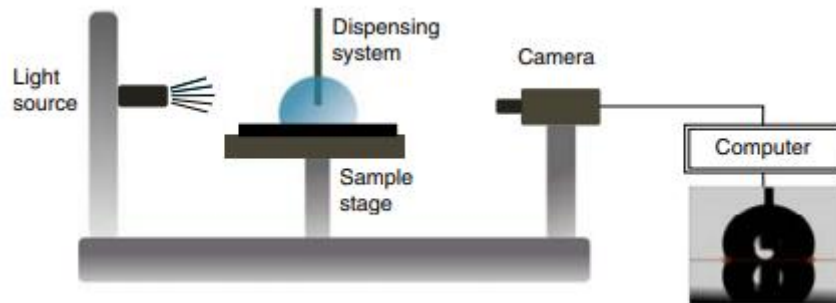
Figure 16. Setup for contact angle analysis (Huhtamäki et al. 2018).

3.2.2 Microscopy

Zeiss Axio Scope A1 microscope was used to analyze the surface of treated and non-treated samples under reflected light to determine whether the treatments and sterilization methods had caused adversely changes to the surfaces. Pictures were taken through a camera connected to the microscope. A scale bar was added to the images using ImageJ software.

3.3 Data analysis

3.3.1 Surface tension

CA graph was plotted in Microsoft Excel for non-sterile, ethanol, ethanol + vortex, autoclaved and UVGI samples. Results were compared to untreated samples, in order to verify if any of the decontamination method affected the treatments applied.

3.3.2 Biofilm quantification

Data generated from SkanIt™ software was exported to Microsoft Excel. Background reading obtained from negative control samples was removed and the average and standard deviation of each sample, in relation to untreated samples, was calculated. Fluorescence unit (FU) values were used to calculate biofilm growth inhibition, relative to untreated controls. FU background of samples alone (negative control) was subtracted from treated samples and percentage of viability was calculated by using Eq. (2).

$$\frac{FU\ treated}{FU\ non-treated} \times 100 \qquad (2)$$

4 RESULTS

4.1 3D printing

Five different sample dimensions were successfully 3D printed for testing (Figure 17). Based on biological assay suitability, the chosen dimension was 10 mm diameter, and height varied according to the applied treatment to the sample (Figure 18).
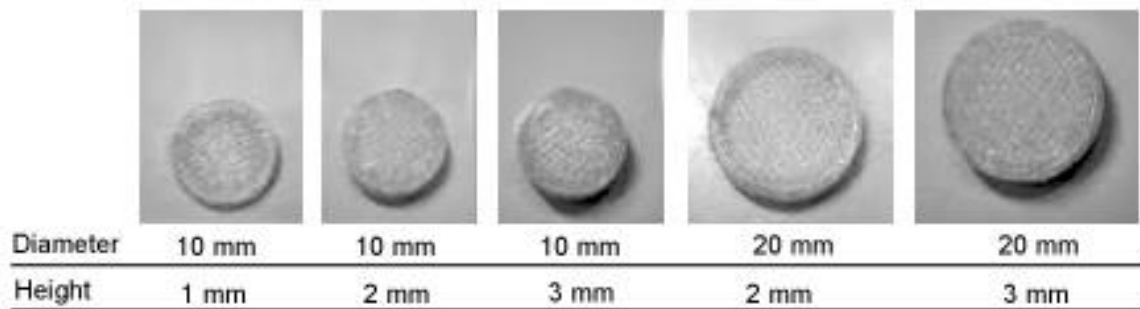
Figure 17. 3D printed samples for testing.
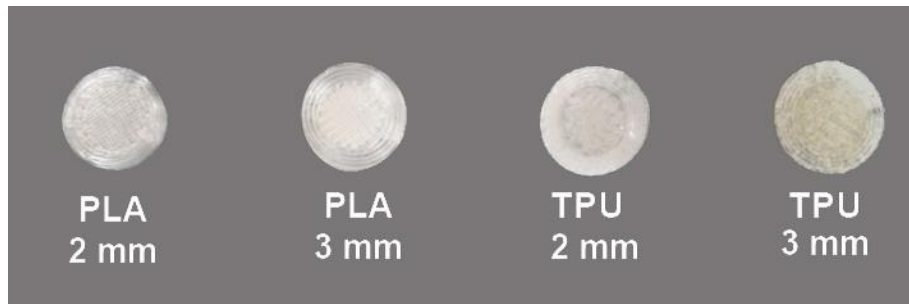
Figure 18. Control samples.

Samples used for surface polishing were 3D printed to the height of 3 mm and ironing feature resulted in smoother PLA and TPU surfaces. However, printing quality of TPU surface was affected by this technique.

4.2 Treatments

4.2.1 Additives

PLA and TPU filaments were treated with PEG and castor oil prior 3D printing of the samples. Treated filaments had an increase in their weight, which indicates that both

materials absorbed the treatments. According to Table 2, it was observed that PEG treated filaments had the highest absorbance, with TPU showing an increase of 16% compared to its original weight.

Table 2. Weight in grams of treated and non-treated filaments

	Non-treated	**Treated with PEG**	**Treated with castor oil**
PLA	4.64 g	5.12 g	4.79 g
TPU	4.28 g	4.97 g	4.56 g

Samples were successfully 3D printed (Figure 19) and presented the same surface quality as non-treated samples. However, during 3D printing process, it was noticed that a few samples varied in height. While samples produced from PEG treated filaments were not affected, those treated with castor oil presented a decrease of 20% in height. The diameter of the samples was not affected.
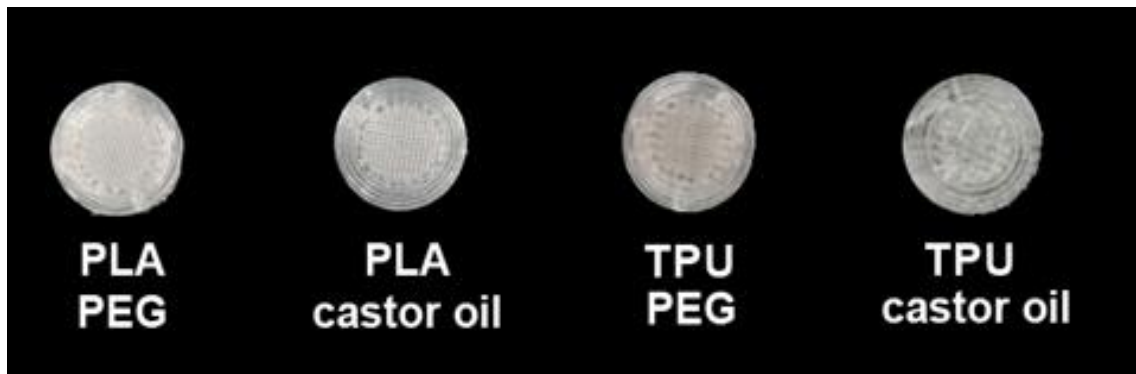
Figure 19. 3D printed samples using additives.

Futhermore, as seen in Figure 20, samples manufactured from treated filaments presented distinct change in transparency compared to non-treated samples. PLA-castor oil and TPU castor oil showed higher transparency, suggesting incorporation of the treatements in the samples.
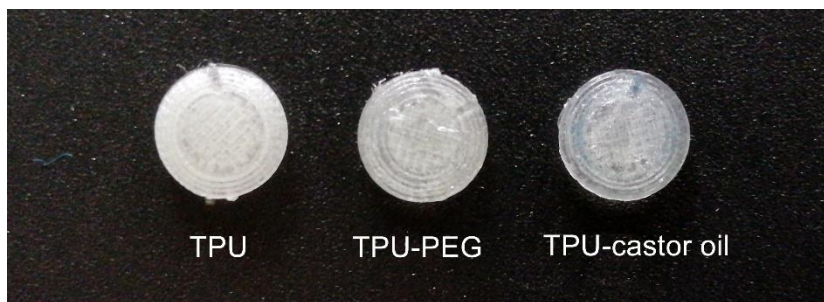
Figure 20. Difference in transparency between samples 3D printed with treated and non-treated filaments.

4.2.2 Surface polishing

Samples produced for surface polishing had their top layer 3D printed using ironing feature to decrease surface roughness. This technique was successfully applied to PLA samples. However, despite decreasing surface roughness of TPU samples, the printing quality of the top layer was compromised (Figure 21).

Figure 21. PLA and TPU 3D printed samples using the ironing feature.

4.3 Surface decontamination

Before the microbiological assays were performed, all samples were submitted to a decontamination step. From the four different decontamination methods tested, two, immersion in 70% ethanol and 70% ethanol with intermittent vortexing, were not efficient in decontaminating polished surfaces. Additionally, PLA 3 mm in the vortexed test tube containing 70% ethanol was turbid – an indicator of bacterial growth (Figure 22).

Figure 22. Bacterial growth on a PLA polished sample.

When samples were submitted to sterilization by autoclavation, all surfaces were successfully decontaminated (Table 3). However, CA measurement results (section 4.4.1) and microscopy analysis (section 4.4.2) indicated that this sterilization process affected the surface of the samples. UVGI showed excellent results by decontaminating all tested samples.

Table 3. Bacterial growth and decontamination methods

Sample	Treatments			
	70% ethanol	70% ethanol + vortex	Autoclave	UVGI
PLA 2 mm	-	-	-	-
PLA and PEG	-	-	-	-
PLA and castor oil	-	-	-	-
PLA 3 mm	-	+	-	-
polished PLA	+	+	-	-
TPU 2 mm	-	-	-	-
TPU and PEG	-	-	-	-
TPU and castor oil	-	-	-	-
TPU 3 mm	-	-	-	-
polished TPU	+	+	-	-

-: no bacterial growth observed; +: bacterial growth observed

4.4 Sample characterization

4.4.1 Surface tension

CA was used to characterize surface hydrophilicity. Due to the limited size of the samples, it was not possible to analyze different measurement points of the surface, so the measurement was done on the same location in triplicate. Uncertainty of 1 µm might lead to 10º difference in the measurement of the CA (Butt et al. 2014 as cited in Vuckovac et al. 2019). Because image resolution may affect the uncertainty of the measurements, only difference above 10º in CA was considered relevant for this study.

Surface tension was analyzed on all samples prior to decontamination process and on samples exposed to autoclave and UVGI. CA was not measured on samples treated with 70% ethanol and 70% ethanol with vortex due to their inefficacy as decontamination methods.

Considering standard deviation, TPU-castor oil and PLA polished samples had a relevant decrease (>10º) in CA, becoming more hydrophilic compared to non-treated samples. However, TPU polished samples had a significant change, by having the CA increase to 10.21º (Table 4).

Control samples 3D printed with ironing feature had a decreasing in their CA compared to a regular 2 mm 3D printed sample. The most notable change was seen in TPU, when the CA decreased by 15.8º when the top layer was printed with ironing.

Table 4. Contact angle of 3D printed samples prior sterilization

Samples	Contact angle	Difference between treated and non-treated samples
PLA 2 mm*	63.73º (±2.2)	-
PLA-PEG	58.61º (±1.3)	-5.12º
PLA-castor oil	58.30º (±2.1)	-5.42º
PLA 3 mm*	58.47º (±3.2)	-
PLA polished	53.43º (±5.9)	-5.04º
TPU 2 mm	91.36º (±2.8)	-
TPU-PEG	91.88º (±1.0)	0.52 º
TPU-castor oil	82.09º (±2.2)	-9.27 º
TPU 3 mm*	75.60º (±1.6)	-
TPU polished	85.81º (±3.5)	10.21º

*Control sample

Figure 23 shows that the two decontamination methods tested affected the surface energies of some 3D printed samples by means of decreasing the CA.

Autoclaved samples decreased CA of PLA 3 mm and TPU 3 mm by 20º and 14º, respectively. Thus, samples surfaces became significantly more hydrophilic. On the other hand, for samples treated with UVGI, a decrease in CA was observed for TPU-PEG and polished TPU (Figure 23) by considerably increasing their surface energies. A decrease of 42º and 15º, respectively in their CA was measured. The remaining samples did not present a significant variation in CA when exposed to UVGI (Figure 23), in relation to non-sterile samples.
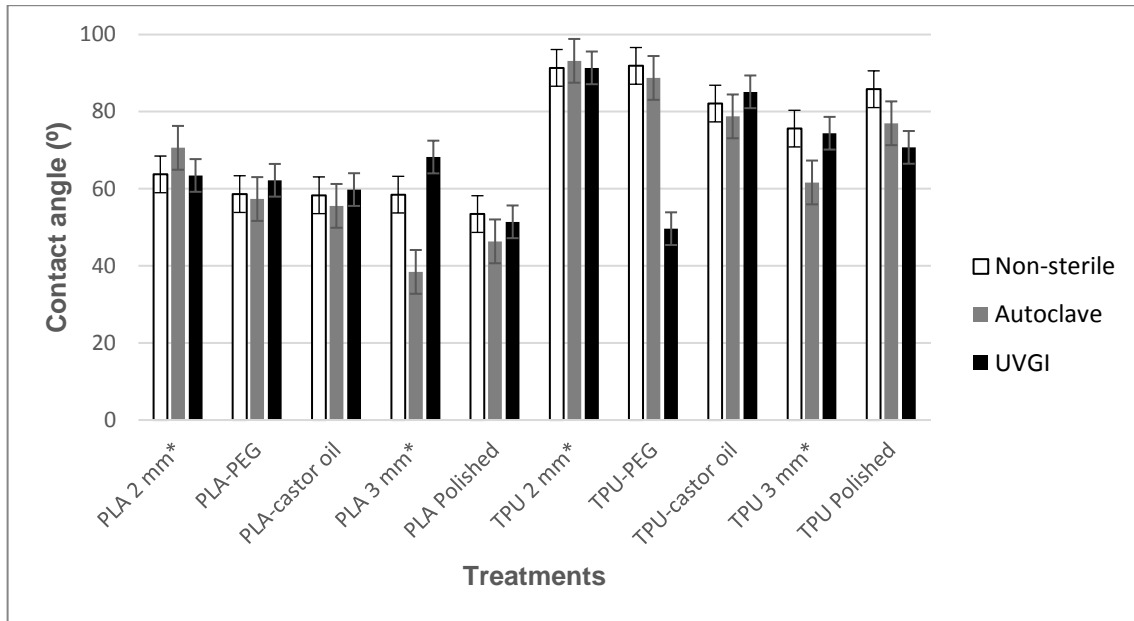
*Control sample

Figure 23. Contact angle of non-sterile, autoclaved and UVGI decontaminated samples.

4.4.2 Microscopy

Samples were analyzed through optical microscopy to verify any changes on the surface after treatments and after decontamination process. The latter was only performed for autoclaved samples. Ethanol failed to decontaminate the samples, thus microscopy analysis not was not performed in those samples. Unfortunately, samples subjected to UVGI could not have their surfaces analyzed microscopically due to suspension of lab activities during coronavirus pandemic.

Microscopy was also used for analysis of surfaces during polishing process. Filament orientation can be observed in Figure 24a, from a TPU sample prior treatment. Surface polishing decreased roughness of both PLA and TPU samples, resulting in a smoother, glossy surface (Figure 24b). However, it was not possible to obtain a scratch-free surface on all samples.

35
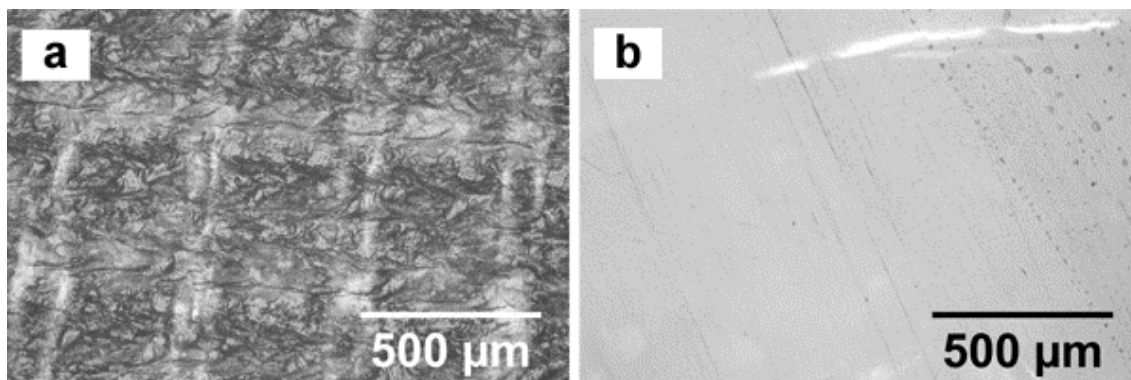
*Figure 24. Optical microscopy of samples prior decontamination: (**a**) non-treated TPU and (**b**) after surface polishing.*

It was macroscopically observed that treated filaments produced more translucid samples. Castor oil treated filaments had the most noticeable transparency change of all treated samples.

Visual inspection showed no shape alteration on autoclaved samples. However, TPU samples presented surface discoloration – an indicator of thermal degradation. Additionally, optical microcopy analysis revealed layer distortion and entrapped air presented in almost all samples (Figure 25b to 25f), with an exception of PLA polished (Figure 25a), that presented erosions on the surface.
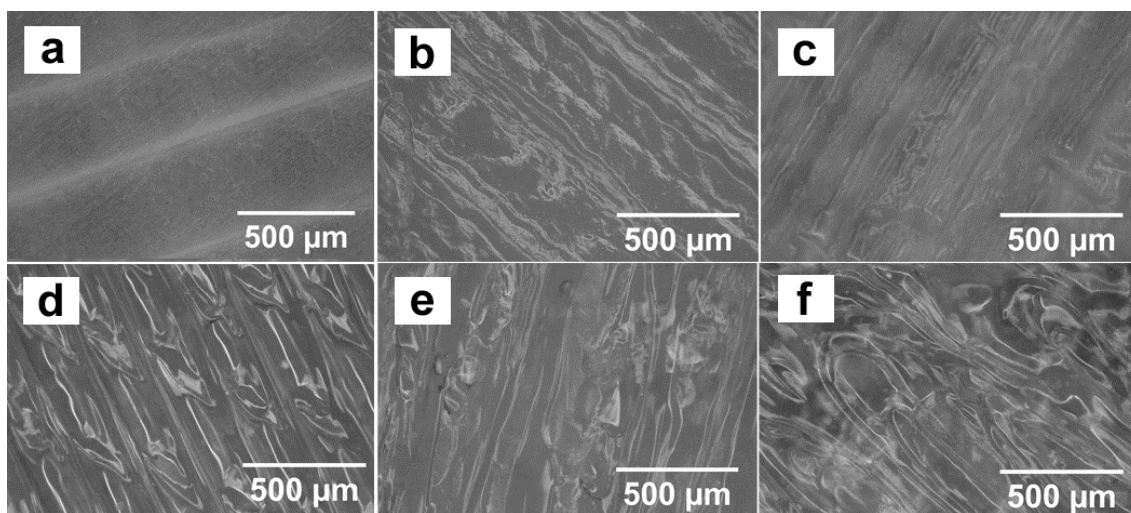
*Figure 25. Microscopy images of autoclaved samples: (**a**) Polished PLA (**b**) PLA-PEG (**c**) PLA-castor oil (**d**) Polished TPU (**e**) TPU-PEG (**f**) TPU-castor oil.*

36

4.5 Biofilm formation inhibition

Only samples that were successfully decontaminated were used in biofilm formation inhibition assays: autoclaved and UVGI, although two control samples (PLA and TPU 3mm) had significant alterations in their wettability and microscopically properties after autoclavation.

Samples sterilized by autoclave were subjected to bacterial biofilm testing in two independent experiments (Figure 26a). In the first assay, PLA-castor oil and PLA-PEG samples were the only ones which showed a minor biofilm reduction, but those samples also presented a high variability within replicates (i.e. 22% (± 8) and 8% (± 36), respectively). In the second assay, polished TPU and polished PLA samples inhibited biofilm formation by 47% (± 6) and 33% (±36), respectively. Based on these preliminary data, polished surfaces may be promising results for biofilm inhibition. Agreeably CA for polished PLA samples was of the lowest obtained.
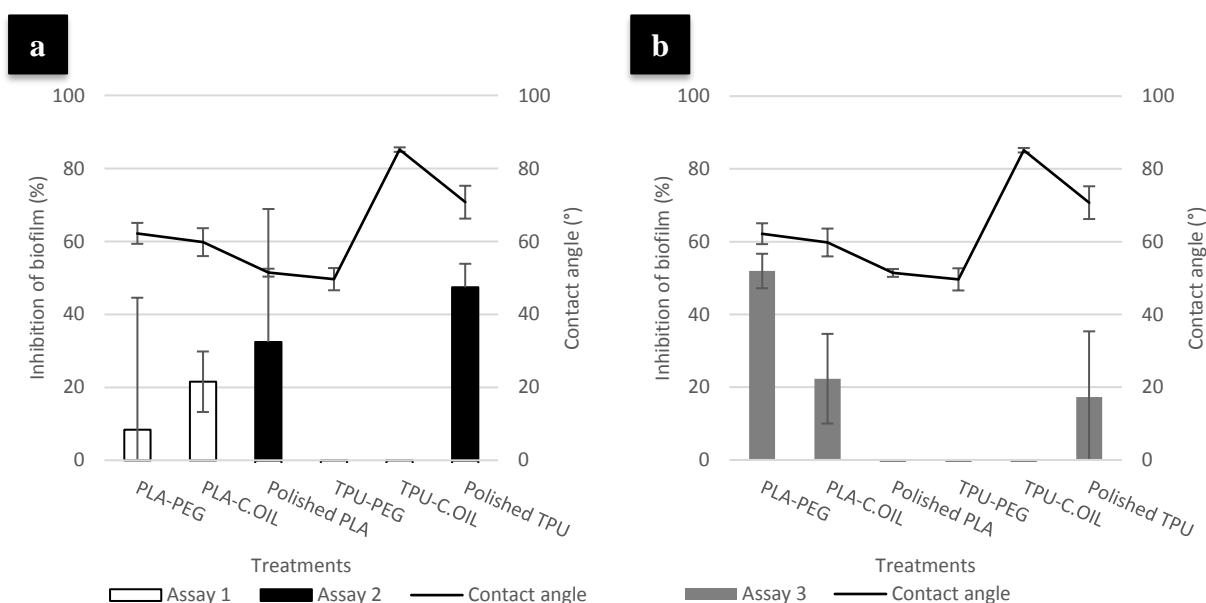
*Figure 26. Inhibition of biofilm formation of (**a**) treated samples sterilized by autoclave (n =2). CA measurements are from Assay 1 (n=3) and (**b**) treated samples decontaminated with UVGI (n =2). CA measurements (n=3).*

Third assay was done after samples were decontaminated using UVGI. PLA-PEG samples resulted in 52% (±5) biofilm inhibition, followed by 22% (±12) in PLA-castor oil and 17% (±18) in polished TPU (Figure 26b). Although polished PLA and TPU-PEG showed the lowest CA values, this did not relate to a decrease in biofilm formation, by the methodology used in our studies. Unfortunately, this assay could not be reproduced due to coronavirus pandemic.

5 DISCUSSION

5.1 3D printing

Samples subjected to surface polishing were 3D printed to the height of 3 mm because as the polishing process removes material, samples would lose approximately one millimeter in thickness. A 3D printed TPU holder was manufactured for this process. Due to its flexibility, samples were easily placed and removed from the holder.

With both PEG and castor oil-treated filaments, the major challenging was to ensure that the loading tube of the printer was cleaned well before changing filaments, so no cross contamination would occur when new samples were being produced. Additionally, clogged extruder nozzle happened often when printing with PLA only filament. Mardis (2018) observed that this happens because PLA expands when heated. Adjusting printing temperature had no effect on clogging. However, PLA-treated filaments had a better flow and no clogs happened.

3D printed control samples had lower CA compared to the literature (Baran and Erbil 2019), with PLA having the most significant difference. This might be due to printing parameters, which became very noticeable when samples were 3D printed with ironing setting (see section 5.2.2).

5.2 Treatments

The treatment procedures done in this study have not been reported in the literature. Therefore, this was an innovative approach. The experiments were carried out based on a combination of different methods found in the literature to lower contact angle of the materials. However, those methods were not executed on 3D printing surfaces.

5.2.1 Additives

PLA and TPU-treated filaments with PEG and castor oil could be easily fed into the loading tube and samples were 3D printed as expected. Although a few samples produced with castor oil could not be used in assays due to not having the appropriated thickness

5.2.2 Surface polishing

Despite the improvements in additive manufacturing technique during the last years, there are limited approaches when it comes to promote surface finish. Very few studies have been conducted on polishing of 3D printed surface. And those studies were on 3D printed metal objects (Iquebal, Sagapuram and Bukkapatnam 2019), which have different morphology and mechanical properties than polymers.

In this study, polishing time was based on constant microscopy analysis during the process to assess surface roughness. Since 3D printed TPU has rougher surface, it required more polishing time than PLA to remove roughness. Even though the rotational speed of the polishing machine could not be adjusted, the speed could be manually decreased by moving the sample to the center of the polishing plate. Friction produced by the polishing process generates heat, which in turn could melt the samples, deforming the surface. Therefore, the use of wet polishing was fundamental to reduce friction.

Microscopy images showed that PLA and TPU 3D printed surfaces presented cracks. It was not possible to obtain a scratch-free surface, since sandpaper introduces small scratches on the surface.

An approach to decrease surface roughness of 3D printing objects is the use of ironing feature. However, only a few 2D slice software has this built-in feature available. During manufacturing, when using the ironing feature, the 3D printer nozzle travels on the top surface and melts the outer layer resulting in a less rough surface, which in turn, increased the surface energy of the material, lowering its CA. TPU sample had a considerable decrease of 15.8° when printed with ironing setting. However, when subjected to polishing treatment, TPU had its CA increased. Nonetheless, it remained lower than the CA of the TPU sample printed without ironing. TPU samples had rougher surface than PLA and therefore, needed to be polished for a little longer, which might have caused the removal of the modified top layer that was made with ironing feature. Thus, the increase in its CA.

5.3 Sample decontamination

3D printed objects are sterile because they are made from extrusion temperatures which leads to significant decrease in biological contaminant load (Neches et al. 2016). However, contamination from the building plate and handling the object does not guarantee that sterility is preserved in the present study. Thus, various methods utilized in biomedical applications were tested in order to find a decontamination method that would cause little to no changes in the CA of the samples.

The expected decontamination results were not achieved with 70% ethanol. Because the samples were light weight, perhaps some of the samples floated instead of sinking in the ethanol solution. Therefore, some samples were not capable to get enough exposure to eliminate the microorganisms present.

The inclusion of a vortexing step to increase fluid dynamics and promote ethanol absorption was also attempted, but not successfully. During a process, such as polishing, microorganisms can easily get trapped in between the surface of the material, making decontamination challenging. Perhaps, pre-cleaning with disinfectant would improve the process (Ribeiro, Neumann, Padoveze and Graziano, 2015). However, the use of cleaning agents could leave residues between the 3D printed layers, interfering with treatments and biofilm assay.

Autoclaving is not recommended for polymers that are not resistant to heat and moisture because thermal degradation might occur (Tipnis and Burgess 2018). Since no literature was found on the effect of autoclave on 3D printed surfaces, this method was carried out to verify if one autoclave cycle would cause significant changes to the samples. According to technical data sheet of PLA and TPU (Appendixes C and D), glass transition temperature for the filaments is 56 ℃ and 138 ℃, respectively. Basing on this, a 15 minutes autoclave cycle at 121 ℃ would have a significant effect on PLA samples and would mostly likely not affect TPU samples. Although autoclavation sterilized all samples, microscopy analysis revealed alterations. Autoclave not only uses heat, but also pressure to kill microorganisms and that could have made a significant change in the structure of the 3D printed polymers, leading to thermal degradation.

The biocide properties of UVGI cited by Chitnis et al. (2008) was confirmed in this study. It was not possible to analyze UVGI decontaminated samples through microscopy to verify surface changes. However, CA analysis showed that surface energy remained similar to most of the control samples prior decontamination than autoclaved ones. Additionally, no signs of thermal degradation were macroscopically seen. Fischbach et al. (2011) noted that PEG-PLA film was successfully sterilized without affecting its structure when exposed to UVGI for 2 hours. However, exposure longer than 5 hours shortened PEG chains. In contrast, a study conducted by Loyaga-Rendon, Iwasaki and Reza (2007) reported that UVGI modifies polymer surface through photochemical changes, resulting in increasing of hydrophilicity. This might have happened to TPU-PEG and TPU polished which had a reduction in their CA compared to non-sterile samples.

5.4 Biofilm inhibition

Biofilm formation on surface of biomedical devices is a complex mechanism that needs to be prevented due to significant morbidity and mortality among patients (Chen et al. 2013). Therefore, the development of polymeric materials that can prevent or weaken bacterial attachment is a promising approach to reduce material-associated biofilm problems (Alves and Pereira cited in Cattò and Cappitelli 2019).

In this study, the biofilm inhibition of *S. aureus* on 3D printed modified materials was investigated. Negative control samples were used as control of sterility process and workflow (media, disks, handling, etc.). It was also used as a background reading during resazurin assay, to adjust for any intrinsic fluorescence produced by the samples themselves.

According to the results, four out of six treated samples showed antibiofilm activity against *S. aureus*. In addition, samples decontaminated with UVGI prior biofilm assays showed better inhibition results compared to autoclaved samples. Research shows that PEG deposited on a surface hinders microorganism attachment (Fernández et al. 2007 as cited in Shah et al. 2013). In agreement with that, PLA-PEG had the most significant antibiofilm properties in this study. It also presented hydrophilic behavior. Unexpectedly, no biofilm inhibition properties were seen in TPU-PEG and TPU-castor oil samples. It

was hypothesized that 3D printing parameters could have negatively affected the additives in TPU filaments, since it was used high temperature to print the samples. Furthermore, considering that it was not possible to control and test the intensity of additive absorption in the filaments, treated filaments with PEG and castor oil might have not produced homogeneous samples, resulting in variation of biofilm inhibition between assays.

6 CONCLUSION

In this thesis, three strategies to decrease the CA of 3D printed samples of PLA and TPU were developed and their effect on biofilm growth of *S. aureus* were evaluated. The steps involved material selection, design, 3D printing, surface treatment, surface characterization, sample decontamination and microbiology assay. Surface tension measurement and microscopy analysis were done in order to verify the integrity of the applied treatments before and after surface decontamination. Prior to decontamination, hydrophilicity was improved on the surface of all samples, except TPU-PEG, which showed no alterations. The most effective decontamination method, based on the sample materials and treatments, was UVGI. Biofilm assays presented different levels of biofilm inhibition. However, PLA-PEG and surface polishing seem to be the most promising biofilm inhibition treatment. Results can be improved by enhancing the methods used for impregnating the treatments to the filaments and optimizing 3D printing settings.

Furthermore, a 3D printed sample holder was manufactured for this work using TPU filament. This opens possibilities for developing new ways to improve polishing technique using FDM.

Despite intense research on biofilm in the last years, creating means for preventing biofilm formation still poses a challenge. Certainly, 3D printing is a promising technology in the medical field. Further research should be conducted in order to understand the implications of modified 3D printed objects and bacterial biofilm inhibition.

REFERENCES

3D@UniPV, n.d., *3D Printed Patches for Esophageal Tissue Engineering*. University of Pavia [online]. Available at: http://www-4.unipv.it/3d/research-activities/3d-printed-patches-for-esophageal-tissue-engineering/ [Accessed: 05 Jan. 2020].

Achinas, S., Charalampogiannis, N. and Euverink, W.G., 2019. A Brief Recap of Microbial Adhesion and Biofilms. *Appl. Sci*. [online], 9(14), 2801. Available at: doi.org/10.3390/app9142801

Aryal, S., 2020, *Light Microscope - definition, principle, types, parts, magnification.* Microbe notes. [online] Available at: https://microbenotes.com/light-microscope/ [Accessed: 30 Apr. 2020].

Baran, H. and Erbil, Y., 2019, Surface Modification of 3D Printed PLA Objects by Fused Deposition Modelling: A Review. *Colloids and Interfaces* 3(2):43.

Bjarnsholt T., 2011, Introduction to biofilms. In: Bjarnsholt T., Jensen P.Ø., Moser C., Høiby N., editors. *Biofilm Infections. Springer*; New York, NY: pp. 1–9.

Brisset, L., Vernet-Garnier, V., Carquin, J., Burde, A., Flament, B. And Choisy, C., 1996, In vivo and in vitro analysis of the ability of urinary catheters to microbial colonization. *Pathol Biol* [online] 44 pp. 397–404. Available at: www.ncbi.nlm.nih.gov/pubmed?cmd=Retrieve&db=PubMed&list_uids=8758484&dopt=Abstract [Accessed: 01 Jan. 2020].

Cattò, C., & Cappitelli, F., 2019, Testing Anti-Biofilm Polymeric Surfaces: Where to Start? *International journal of molecular sciences* [online] 20(15), 3794. Available at: doi:10.3390/ijms20153794 [Accessed: 07 Jan. 2020].

Chemaly, R., Sharma, P., Youssef, S., Gerber, D., Hwu, P., Hanmod, S., Jiang, Y., Hachem, R. and Raad, I., 2010. The efficacy of catheters coated with minocycline and rifampin in the prevention of catheter-related bacteremia in cancer patients receiving high-dose interleukin-2. *International Journal of Infectious Diseases*, 14(7), pp.e548-e552.

Chen M., Yu Q., Sun H., 2013, Novel strategies for the prevention and treatment of biofilm related infections. *International Journal of Molecular Science* [online] 14(9):18488–18501. Available at: doi.org/10.3390/ijms140918488 [Accessed: 01 Jan. 2020].

Chitnis, D., Katara, G., Hemvani, N., Chitnis, S. and Chitnis, V., 2008. Surface disinfection by exposure to germicidal UV light. *Indian Journal of Medical Microbiology*, 26(3), p.241.

Chu, V., Crosslin, D., Friedman, J., Reed, S., Cabell, C., Griffiths, R., Masselink, L., Kaye, K., Corey, G., Reller, L., Stryjewski, M., Schulman, K. and Fowler, V., 2005. Staphylococcus aureus bacteremia in patients with prosthetic devices: Costs and outcomes. *The American Journal of Medicine*, 118(12), p.1416.e23.

Cruz, C., Shah, S. and Tammela, P., 2018. Defining conditions for biofilm inhibition and eradication assays for Gram-positive clinical reference strains. *BMC Microbiology*, 18(1).

Di Ciccio, P., Vergara, A., Festino, A., Paludi, D., Zanardi, E., Ghidini, S. and Ianieri, A., 2015. Biofilm formation by Staphylococcus aureus on food contact surfaces: Relationship with temperature and cell surface hydrophobicity. *Food Control*, 50, pp.930-936.

Dimitrov, D., Schreve, K. and de Beer, N., 2006, Advances in three dimensional printing – state of the art and future perspectives. *Rapid Prototyping Journal*, [online] Vol. 12 No. 3, pp. 136-147. Available at: doi.org/10.1108/13552540610670717 [Accessed: 01 Jan. 2020].

Donlan, R. and Costerton, J., 2002. Biofilms: Survival Mechanisms of Clinically Relevant Microorganisms. *Clinical Microbiology Reviews*, 15(2), pp.167-193.

Fischbach, C., Tessmar, J., Lucke, A., Schnell, E., Schmeer, G., Blunk, T. and Göpferich, A., 2001. *Does UV irradiation affect polymer properties relevant to tissue engineering?*. Surface Science, 491(3), pp.333-345.

Ford, S. and Despeisse, M., 2016, *Additive manufacturing and sustainability: an exploratory study of the advantages and challenge*s [online] ScienceDirect. Available at:

https://www.sciencedirect.com/science/article/pii/S0959652616304395 [Accessed: 24 Dec. 2019].

FormFutura, n.d., *Phyton Flex* [online] Available at: www.formfutura.com/shop/product/python-flex-clear-1037?category=196 [Accessed: 22 Mar. 2020].

Francolini, I. and Donelli, G., 2010, Prevention and control of biofilm-based medical-device-related infections. *FEMS Immunology & Medical Microbiology* [online] Volume 59, Issue 3, pp 227-238. Available at: doi.org/10.1111/j.1574-695X.2010.00665.x [Accessed: 01 Jan. 2020].

Gianfrancesco, A., 2017, Technologies for chemical analyses, microstructural and inspection investigations. [online] ScienceDirect. Available at: www.sciencedirect.com/science/article/pii/B9780081005521000087?via%3Dihub [Accessed: 15 Dec. 2019].

Hoffman, L.R., D'Argenio, D.A., MacCoss, M.J., Zhang, Z., Jones, R.A. and Miller, S.I., 2005, Aminoglycoside antibiotics induce bacterial biofilm formation. *Nature* 436:1171–1175.

Huhtamäki, T., Tian, X., Korhonen, J. and Ras, R., 2018, Surface-wetting characterization using contact-angle measurements. *Nature Protocols,* [online] 13. Available at: https://users.aalto.fi/~rras/publications/111.pdf [Accessed: 17 Apr. 2020].

Iquebal, A., Sagapuram, D. and Bukkapatnam, S., 2019. Surface plastic flow in polishing of rough surfaces. *Scientific Reports*, [online] 9(1). Available at: www.ncbi.nlm.nih.gov/pmc/articles/PMC6650475/#CR12 [Accessed: 26 Apr 2020].

Katsikogianni M. and Missirlis Y.F., 2004, Concise review of mechanisms of bacterial adhesion to biomaterials and of techniques used in estimating bacteriamaterial interactions. *European Cells and Materials,* 8 p 38.

Kazuhisa, M., 2002. *Surface Characterization Techniques: An Overview*. [online] Available at: https://ntrs.nasa.gov/archive/nasa/casi.ntrs.nasa.gov/20020070606.pdf [Accessed: 09 Apr. 2020].

Kerns, J., 2019, *The Challenge of 3D Printing Medical Devices*. [online] MachineDesign. Available at: https://www.machinedesign.com/3d-printing-cad/article/21838078/the-challenge-of-3d-printing-medical-devices [Accessed: 06 Jan. 2019].

Khatoon, Z., McTiernan, C. D., Suuronen, E. J., Mah, T. F., & Alarcon, E. I., 2018, Bacterial biofilm formation on implantable devices and approaches to its treatment and prevention. *Heliyon*, [online] 4(12). Available at:10.1016/j.heliyon.2018.e01067 [Accessed: 01 Jan. 2020].

Krüss, n.d., *Contact Angle* [online] Available at: https://www.kruss-scientific.com/services/education-theory/glossary/contact-angle/ [Accessed: 29 Dec. 2019].

Liu, Z., Wang, Y., Wu, B., 2019, A critical review of fused deposition modeling 3D printing technology in manufacturing polylactic acid parts. *The International Journal of Advanced Manufacturing Technology,* Vol. 102, pp. 2877–2889 doi:10.1007/s00170-019-03332-x

Loyaga-Rendon, P., Takahashi, H., Iwasaki, N. and Reza, F., 2007. Effect of Ultraviolet Light Irradiation on Bonding of Experimental Composite Resin Artificial Teeth. *Dental Materials Journal*, 26(6), pp.805-813.

Mardis, N., 2018. Emerging Technology and Applications of 3D Printing in the Medical Field. *Missouri Medicine*, [online] 115(4). Available at: https://www.ncbi.nlm.nih.gov/pmc/articles/PMC6140256/ [Accessed: 4 May 2020].

Monroe, D., 2007, Looking for chinks in the armor of bacterial biofilms. *PLoS Biol*, [online] 5. Available at: journals.plos.org/plosbiology/article?id=10.1371/journal.pbio.0050307 [Accessed: 25 Dec. 2019].

Namen, F., Galan Jr., J., Oliveira, J., Cabreira, R., Costa e Silva Filho, F., Souza, A. and Deus, G., 2008. Surface properties of dental polymers: measurements of contact angles, roughness and fluoride release. *Materials Research*, 11(3), pp.239-243.

Neches, R. Y., Flynn, K. J., Zaman, L., Tung, E., and Pudlo, N., 2016. On the intrinsic sterility of 3D printing. *PeerJ*, [online] 4, e2661. Available at: doi:10.7717/peerj.2661 [Accessed: 06 Jan. 2020].

Noorisafa, F., Razmjou, A., Emami, N., Low, Z., Korayem, A. and Kajani, A., 2016. Surface modification of polyurethane via creating a biocompatible superhydrophilic

nanostructured layer: role of surface chemistry and structure. *Journal of Experimental Nanoscience*, 11(14), pp.1087-1109.

Omnexus n.d., Complete Guide on Thermoplastic Polyurethanes (TPU). [online] Available at: https://omnexus.specialchem.com/selection-guide/thermoplastic-polyurethanes-tpu [Accessed: 18 Apr. 2020].

Otto, M., 2018. Staphylococcal Biofilms. *Microbiology Spectrum*, 6(4).Percival, S., Suleman, L., Vuotto, C. and Donelli, G., 2015, Healthcare-associated infections, medical devices and biofilms: risk, tolerance and control. Journal of Medical Microbiology [online] 64, pp. 323–334. Available at: www.microbiologyresearch.org/docserver/fulltext/jmm/64/4/323_jmm000032.pdf?expires=1577912026&id=id&accname=guest&checksum=9A6BCF855A4C02ECD8C19C171871057F [Accessed: 01 Jan. 2020].

Ouyang, P., Kang, Y., Yin, G., Huang, Z., Yao, Y. and Liao, X., 2009. Fabrication of hydrophilic paclitaxel-loaded PLA-PEG-PLA microparticles via SEDS process. *Frontiers of Materials Science in China*, 3(1), pp.15-24.

Polívková, M., Hubáček, T., Staszek, M., Švorčík, V. and Siegel, J., 2017. Antimicrobial Treatment of Polymeric Medical Devices by Silver Nanomaterials and Related Technology. *International Journal of Molecular Sciences*, 18(2), p.419.

Rajan, K., Al-Ghamdi, A., Parameswar, R. and Nando, G., 2013. Blends of Thermoplastic Polyurethane and Polydimethylsiloxane Rubber: Assessment of Biocompatibility and Suture Holding Strength of Membranes. *International Journal of Biomaterials*, 2013, pp.1-7.

Räsänen, S., 2018. *A catheter coated with antimicrobial peptides saves you from healthcare-associated infections*. [online] University of Oulu. Available at: https://www.oulu.fi/university/node/55552 [Accessed: 30 Dec. 2019]

Ribeiro, M., Neumann, V., Padoveze, M. and Graziano, K., 2015. Efficacy and effectiveness of alcohol in the disinfection of semi-critical materials: a systematic review. *Revista Latino-Americana de Enfermagem*, [online] 23(4), pp.741-752. Available at: http://www.ncbi.nlm.nih.gov/pmc/articles/PMC4623738/ [Accessed: 27 Apr. 2020].

Sin, L. and Tueen, B., 2019. *Polylactic Acid: A Practical Guide for the Processing, Manufacturing, and Applications of PLA*. 2nd ed. San Diego: Elsevier Science & Technology Books, p.53.

Shah, S., Tatara, A., D'Souza, R., Mikos, A. and Kasper, F., 2013. Evolving strategies for preventing biofilm on implantable materials. *Materials Today*, 16(5), pp.177-182.

Singhvi, M.S., Zinjarde, S.S. and Gokhale, D.V., 2019, *Polylactic acid: synthesis and biomedical applications*. Journal of Applied Microbiology ISSN 1364-5072

Tipnis, N. and Burgess, D., 2018. Sterilization of implantable polymer-based medical devices: A review. *International Journal of Pharmaceutics*, 544(2), pp.455-460.

Villani, M., Consonni, R., Canetti, M., Bertoglio, F., Iervese, S., Bruni, G., Visai, L9., Iannace, S. and Bertini, F., 2020. Polyurethane-Based Composites: Effects of Antibacterial Fillers on the Physical-Mechanical Behavior of Thermoplastic Polyurethanes. *Polymers*, [online] 12(2), p.362. Available at: www.ncbi.nlm.nih.gov/pmc/articles/PMC7077423/ [Accessed: 26 Apr. 2020].

Vizzeswarapu, P., 2014, *Plastic to smile about - thermoplastic polyurethane*. Medical Devices Development [online]. Available at: https://www.medicaldevice-developments.com/features/featureplastic-to-smile-about---thermoplastic-polyurethane-4454777/ [Accessed: 18 April 2020]. Medical Devices Development, [online] Available at: www.medicaldevice-developments.com/features/featureplastic-to-smile-about---thermoplastic-polyurethane-4454777/ [Accessed: 18 Apr. 2020].

Vuckovac, M., Latikka, M., Liu, K., Huhtamäki, T. and Ras, R., 2019. Uncertainties in contact angle goniometry. *Soft Matter*, [online] 15(35), pp.7089-7096. Available at: https://pubs.rsc.org/en/content/articlelanding/2019/sm/c9sm01221d#!divAbstract [Accessed: 23 April 2020].

Young, T., 1805. *An Essay on the Cohesion of Fluids*. Phil. Trans. R. Soc. London, p. 95.

Xiao, J. and Gao, Y., 2017. The manufacture of 3D printing of medical grade TPU. *Progress in Additive Manufacturing*, 2(3), pp.117-123.

Zisman, W., 1964, Relation of the Equilibrium Contact Angle to Liquid and Solid Constitution. *Advances in Chemistry*, [online] 43. Available at: https://pubs.acs.org/doi/pdf/10.1021/ba-1964-0043.ch001?src=recsys [Accessed: 23 Dec. 2019].

APPENDIX A – CONTACT ANGLES

Samples	Treatments	Contact angle of non-sterile samples			Average	Standard deviation	Difference in treated and non-treated samples (%)
Non-sterile	PLA 2 mm**	66.30	60.92	63.97	63.73	2.20	-
	PLA-PEG	58.60	60.26	56.97	58.61	1.34	8.03
	PLA-castor oil	56.30	61.20	57.40	58.30	2.09	8.52
	PLA 3 mm**	62.69	57.81	54.90	58.47	3.21	-
	PLA polished	61.76	48.39	50.14	53.43	5.93	8.61
	TPU 2 mm**	94.96	88.09	91.02	91.36	2.81	-
	TPU-PEG	90.44	92.84	92.35	91.88	1.03	-0.57
	TPU-Castor oil	85.25	80.50	80.53	82.09	2.23	10.14
	TPU 3 mm**	73.71	75.47	77.61	75.60	1.59	-
	TPU polished	90.00	85.96	81.48	85.81	3.48	-13.51
Autoclaved	PLA 2 mm**	73.70	66.05	72.10	70.62	3.29	-
	PLA-PEG	61.29	55.09	55.62	57.33	2.81	18.81
	PLA-castor oil	46.36	59.18	61.13	55.56	6.55	21.33
	PLA 3 mm**	39.06	38.85	37.38	38.43	0.75	-
	PLA polished	45.36	45.89	47.80	46.35	1.05	-20.61
	PU 2 mm**	93.43	92.40	93.71	93.18	0.56	-
	TPU-PEG	85.09	89.21	91.95	88.75	2.82	4.75
	TPU-castor oil	78.27	78.37	79.68	78.77	0.64	15.46
	TPU 3 mm**	60.98	61.66	62.26	61.63	0.52	-
	TPU polished	77.25	77.25	76.44	76.98	0.38	-24.90
UVGI	PLA 2 mm**	63.01	61.58	65.75	63.45	1.73	-
	PLA-PEG	65.09	63.20	58.29	62.19	2.86	1.98
	PLA-castor oil	64.64	59.41	55.3	59.78	3.82	5.77
	PLA 3 mm**	64.69	78.00	62.00	68.23	6.99	-
	PLA polished	51.07	52.89	50.30	51.42	1.08	24.64
	TPU 2 mm**	94.96*	88.09*	91.02*	91.36*	2.81*	-
	TPU-PEG	46.99	53.91	48.02	49.64	3.05	45.66
	TPU-castor oil	84.96	85.97	84.49	85.14	0.62	6.80
	TPU 3 mm**	71.93	70.13	81.15	74.40	4.83	-
	TPU polished	74.81	72.92	64.46	70.73	4.50	4.94

* From another set of data (Contact angle of 3D printed samples prior decontamination)

** Control sample

APPENDIX B – FLUORESCENCE UNITS FROM BIOFILM ASSAYS

Assay 1 – Samples sterilized by autoclave

RFU	PLA-PEG	PLA-C.OIL	Polished PLA	TPU-PEG	TPU-C.OIL	Polished TPU
Treated	398.3	593.2	725.3	594.5	483.9	583.1
	404.9	590.6	749.9	603.5	490.9	571.6
	731.3	490.3	618.4	503.2	564.8	579.3
	743.3	499.7	614.7	501.1	549.1	558.9
Untreated (Control)	PLA 2 mm	PLA 2 mm	PLA 3 mm	TPU 2 mm	TPU 2 mm	TPU 3 mm
	591.6	612.0	688.3	494.4	458.7	577.5
	597.0	606.5	680.7	497.2	449.9	575.0
Neg. Ctrl (Background)	PLA-PEG	PLA-C.OIL	Polished PLA	TPU-PEG	TPU-C.OIL	Polished TPU
	116.6	114.6	115.2	113.0	113.5	114.0
	113.8	111.6	112.7	111.4	111.6	113.1

Assay 2– Samples sterilized by autoclave

RFU	PLA-PEG	PLA-C.OIL	Polished PLA	TPU-PEG	TPU-C.OIL	Polished TPU
Treated	140.3	154.7	264.3	209.8	150.8	157.3
	171.6	154.9	271.0	202.5	157.5	144.3
	134.9	258.1	114.5	150.7	192.9	132.6
	139.5	260.4	104.9	118.5	164.9	125.9
Untreated (Control)	PLA 2 mm	PLA 2 mm	PLA 3 mm	TPU 2 mm	TPU 2 mm	TPU 3 mm
	125.5	205.1	252.5	125.5	131.7	228.0
	145.6	182.6	265.8	121.8	134.1	227.9
Neg. Ctrl (Background)	PLA-PEG	PLA-C.OIL	Polished PLA	TPU-PEG	TPU-C.OIL	Polished TPU
	41.70	41.76	41.86	41.89	40.44	42.77
	40.38	41.34	42.10	41.66	41.07	42.21

Assay 3 – Samples decontaminated with UVGI

RFU	PLA-PEG	PLA-C.OIL	Polished PLA	TPU-PEG	TPU-C.OIL	Polished TPU
Treated	66.48	89.62	156.6	89.42	84.70	93.35
	70.66	91.48	143.9	81.39	79.51	91.65
	61.76	79.81	133.2	96.01	90.95	72.37
	62.49	70.74	123.5	79.22	89.51	68.13
Untreated (Control)	**PLA 2 mm**	**PLA 2 mm**	**PLA 3 mm**	**TPU 2 mm**	**TPU 2 mm**	**TPU 3 mm**
	104.0	93.85	68.80	72.48	57.82	90.89
	104.6	102.1	73.75	70.74	58.50	93.30
Neg. Ctrl (Background)	**PLA-PEG**	**PLA-C.OIL**	**Polished PLA**	**TPU-PEG**	**TPU-C.OIL**	**Polished TPU**
	28.66	31.10	29.10	52.00	39.27	30.54
	29.95	29.98	29.67	49.37	39.35	29.42

APPENDIX C – PYTON FLEX® TECHNICAL DATA SHEET

Technical Data Sheet

Product name: **Python Flex**

Python Flex is a high-performance flexible thermoplastic polyurethane (TPU) filament, which is designed for high speed printing on both direct drive and Bowden style extruders. Python Flex is an extremely easy to print flexible filament which can be printed directly on a glass plate without having to use the heatbed.

Python Flex has a shore hardness of 98A and has great elastic properties as allows itself to be stretched up to 450% before breaking. Python Flex is extremely transparent in its natural form and has excellent resistance to oil, greases, microorganisms and abrasion.

Properties	Typical value	Test Method	Test condition
Physical			
Specific gravity	1.16 g/cc	ISO 1183	-
Melt flow rate	-	-	-
Water absorption	-	-	
Moisture absorption			
Mechanical			
Impact strength	No Break	ISO 179	Charpy Notched @23° C (73° F)
Tensile strength	50.0 Mpa	ISO 527 1/2	@Yield
Tensile modulus	150 Mpa	ISO 527	-
Elongation at break	450%	ISO 527 1/2	-
Flexural strength	-	-	-
Flexural modulus	-	-	Shore A Hardness
Hardness	98A	ISO 7619-1	
Thermal			
Print temperature	± 220 - 250° C	-	-
Melting termperature	± 220 ± 10° C	-	-
Viscat softening temp.	± 138° C	ASTM D1525	B/2 (120° C/h, 50N)
Optical			
Haze	-	-	-
Transmittance	-	-	-
Gloss			-

Product details, certifications and compliance	
HS Code	39169090
REACH compliant	Yes
RoHS certified	Yes

Diameter	Tolerance	Roundness
1.75mm	± 0.05mm	≥ 95%
2.85mm	± 0.10mm	≥ 95%

APPENDIX D – BQ EASYGO PLA TECHNICAL DATA SHEET

PLA Filament 1.75 mm
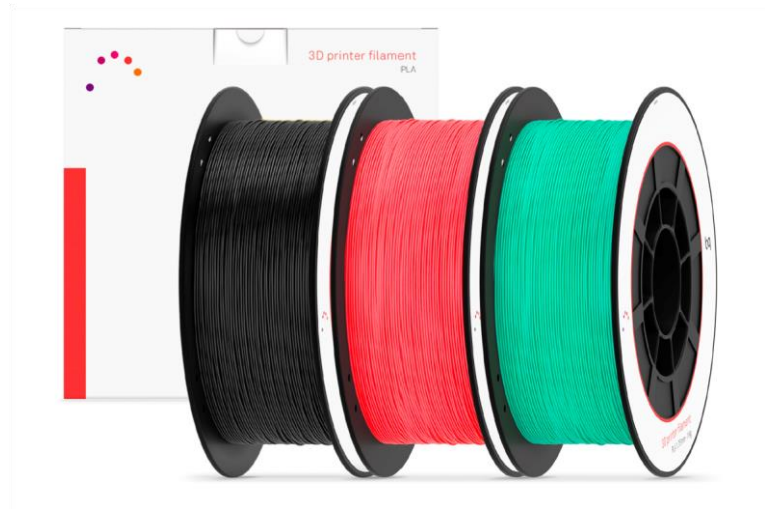
PLA (Polylactic acid) is the best material for getting started with your 3D printer, as it:

– Hardens quickly

– Has minimal thermal tension

– Has minimal deformation

– Does not require Kapton tape

– Does not require heated bed

– Acetone-resistant

BQ PLA filament is made from 100% PLA.

PLA is a biodegradable product obtained from plant-derived sugars.

Flexural elastic modulus: 3600 MPa (ISO 178)

Flexural strength: 108 MPa (ISO 178)

Hardness: 85 Sh D (ASTM D2240)

	Injection-moulded	Printed	
		test pieces[1]	test pieces[2]
Tensile strength at break[*]	52 MPa	50 MPa	39 MPa
Tensile elongation at break[*]	5%	9%	4%
Tensile modulus[*]	1320 MPa	1230 MPa	1120 MPa

[1] Stretched parallel to layers
[2] Stretched perpendicular to layers [*] ISO 527

Filament Diameter: 1.75 mm

Thickness: 1.24 g/cm³ (ASTM D792)

Recommended printing temperature: 200/220 ºC

Heat distortion temperature: 56 ºC (ISO 75/2B)

Weight: 1 kg

Spool Size: 195 mm x 73 mm

Melting temperature: 145/160 ºC (ASTM D3418)

Glass Transition Temperature: 56/64 ºC (ASTM D3418)

Compatible with: any printer that uses 1.75 mm filament

bq